

# RESULTS OF THE HIGH RESOLUTION OTR MEASUREMENTS AT KEK AND COMPARISON WITH SIMULATIONS\*

B. Bolzon<sup>#1,2,3</sup>, T. Lefevre<sup>1</sup>, S. Mazzoni<sup>1</sup>, C. P. Welsch<sup>2,3</sup>, P. Karataev<sup>4</sup>, K. Kruchinin<sup>4</sup>, A. Aryshev<sup>5</sup>  
CERN, Geneva, Switzerland<sup>1</sup>  
Cockcroft Institute, Warrington, Cheshire, U.K.<sup>2</sup>  
The University of Liverpool, Liverpool, U.K.<sup>3</sup>  
J.A.I. at Royal Holloway, University of London, Egham, Surrey, U.K.<sup>4</sup>  
KEK, Tsukuba, Ibaraki, Japan<sup>5</sup>

## *Abstract*

Optical Transition Radiation (OTR) is emitted when a charged particle crosses the interface between two media with different dielectric properties. It has become a standard tool for beam imaging and transverse beam size measurements. At the KEK Accelerator Test Facility 2 (ATF2), OTR is used at the beginning of the final focus system to measure micrometre beam size using the visibility of the OTR Point Spread Function (PSF). In order to study in detail the PSF and improve the resolution of the monitor, a novel simulation tool has been developed. Based on the physical optic propagation mode of ZEMAX, the propagation of the OTR electric field can be simulated very precisely up to the image plane, taking into account aberrations and diffraction. This contribution presents the comparison between Zemax simulations and measurements performed at ATF2.

## INTRODUCTION

Beam imaging systems very often require a number of optical elements to transport the emitted radiation to the light detection system or camera. Different optical errors are introduced by any such elements, which can all cause a degradation of the final resolution and thus the accuracy of the beam measurement. The resolution of an optical system is normally defined as the root-mean-square size of the PSF, defined as the image of the field generated by a single particle, which is the response of the instrument to an elementary source. Therefore, the PSF contains information about both, the actual source distribution at the target surface and imperfections of the optical system. An optimised imaging system would provide a resolution limited by diffraction only.

The resolution of transition radiation imaging systems has been extensively studied for high resolution monitoring using diffraction laws [1-3]. However, the most advanced analytical calculations developed to study the PSF propagate the spatial distribution of radiation sources for a single particle or for a perfect Gaussian beam through ideal lenses up to the image plane. Main sources of errors are not correctly taken into account in these models and the PSF can thus not be calculated precisely this way. The first experimental investigations

of the OTR PSF have been carried at the KEK-ATF2 facility using extremely low emittance electron beams [4] [5]. In the initial set-up chromatical and spherical aberrations were observed and limited the resolution of the beam size monitors. A new software tool is being currently developed that shall allow for a realistic simulation of the OTR PSF. In this paper, we present the result of simulation tool and their application to the optimisation of the high resolution OTR imaging system under development at ATF2.

## SIMULATION TOOL

### *Design Specifications*

One of most important parameter in simulating the PSF of an OTR imaging system resides in the exact description of the source, i.e. OTR field emitted by a single particle. The large tails of an OTR transverse distribution give a significant contribution to the PSF when propagating through a narrow aperture due to diffraction and aberrations [6], and they have thus to be simulated very accurately. When simulating radiation from relativistic particles, the optical elements are located in most cases at distances from the source that are small enough so that near field conditions must be considered [7] [8]. Finally, the simulation tool must be able to reproduce errors given by misalignments or depth of field (from e. g. a 45° OTR screen), which will quantify the required optical and mechanical tolerances when designing and installing the optical system.

### *Simulation of the OTR PSF using Zemax*

Zemax is a widely used optical and illumination design software which can perform standard sequential ray tracing through optical elements, non-sequential ray tracing for analysis of stray light, and physical optics propagation (POP) [9]. While the ray-tracing tool is commonly used to calculate the aberrations of a given optical system, it fails to provide accurate predictions for collimated beams or when the light propagation length is long compared to the dimensions of the optical system. This unfortunately corresponds to experimental conditions commonly reached in high-energy beam imaging system. Alternatively, POP propagates, using diffraction laws, the wavefront of any light source through arbitrary optical lines, taken into account all

#Benoit.Bolzon@cern.ch

optical errors including diffraction, geometrical and chromatic aberrations, depth of field and misalignment.

The equation of the OTR electric field at the source for vertical ( $E_y$ ) polarization component induced by a single electron on a target surface is given as follows [10]:

$$E_y = const \frac{y}{Z} \left[ \frac{2\pi}{\gamma\lambda} K_1 \left( \frac{2\pi}{\gamma\lambda} Z \right) - \frac{J_0 \left( \frac{2\pi}{\lambda} Z \right)}{Z} \right]$$

with  $Z = \sqrt{x^2 + y^2}$ ,  $x = \rho \cos(\varphi)$  and  $y = \rho \sin(\varphi)$  are two orthogonal coordinates of the target measured from the point of electron incidence,  $\rho$  and  $\varphi$  are the polar coordinates,  $\gamma$  is the charged particle Lorentz factor,  $\lambda$  is the radiation wavelength,  $K_1$  is the first order modified Bessel function,  $J_0$  is the zero order Bessel function.

A comparison between analytical calculations and Zemax simulations of optical transition and diffraction in free space propagation is presented here [11]. In the case discussed in this paper, the OTR field is propagating through an imaging system that includes the viewport, mirrors and lenses. With an extremely small vertical beam emittance, the typical beam size in ATF2 has a flat shape with much larger horizontal beam size and the vertical beam size reaches dimensions of the order of few microns. The only way to measure such small size using OTR is to measure the visibility of the PSF of vertically polarised OTR photons [4]. Experimentally a polariser is used to select the photons accordingly whereas in simulations only the vertically polarised photons are taken into account.

## EXPERIMENT AND SIMULATION

KEK-ATF is a 1.28GeV damping ring which produces an extremely low emittance beam. The particles are then extracted from the ring and sent through a transfer line built to study the final focussing scheme of future linear colliders. The OTR system at ATF2 has been integrated into the laser wire system and a complete description of the system can be found in [12]. The imaging system has been recently modified to minimise the PSF size by reducing geometrical and chromatic aberrations. The optic is still based on single-lens, which has been mounted on a motorised XY translation stage to be able to carefully adjust its transverse position. From simulations, the diameter of the lenses, initially 50.8mm, has been decreased down to 30mm to minimise aberrations without adding diffraction.

We experimentally compared the images generated by two types of lenses, one 100mm focal length plano-convex lens (SLB-30-100-PY2 from Sigma-Koki) similar to the lens used in the previous experiment and one 120mm focal length achromat doublet lens (DLB-30-120-PM from Sigma-Koki). A large magnification was chosen for both lenses (respectively  $M=9.13$  and  $M=7.39$ ). A set of optical filters was used (500nm with 25nm and 40nm bandwidth, 550nm with 25nm and 40nm bandwidth and 600nm with 40nm bandwidth) in order to study chromatic

effects and to measure how the PSF changes for different wavelengths. A remotely controlled iris has also been inserted one centimetre upstream of the lens to study spherical aberration and diffraction effects.

Each lens has been tested with similar beam conditions (beam charge and energy) and using a test procedure described as follows:

- Adjusting the longitudinal position of the lens to find the best focus
- Rotating the polarizer to select only vertically polarized photons
- Adjusting the vertical height of the lens to minimise misalignment
- Adjusting the quadrupole strength to get the smallest beam size
- Changing the iris diameter to minimise the PSF

### Best Focus

In order to find the best focus on the camera, the lens is moved longitudinally by step of 100 $\mu$ m thanks to a stepping motor. Experimentally, the best focus is found when the distance between the two peaks of the main lobes is minimised. The distances between the OTR target and the lens and between the lens and the CCD camera can only be measured within few mm accuracy. Thus the longitudinal position of the lens in simulations is moved around the paraxial focal distance of the lens (herein referred as ‘‘paraxial focus’’) in order to find a magnification (distance between the two peaks) similar to what is measured experimentally at best focus.

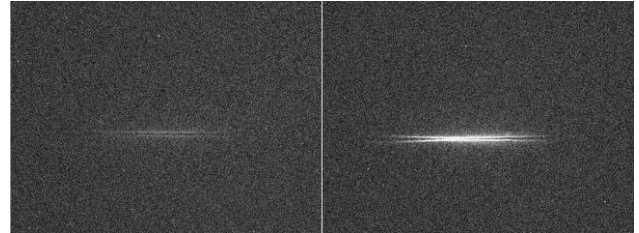


Figure 1: PSF images obtained with SLB-30-100-PY2 (left) and with DLB-30-120-PM (right).

Figure 1 shows the images of the PSF measured at best focus for the plano-convex and the achromat doublet lenses respectively on the left and the right sides. Figures 2 and 3 show the vertical projections for both lenses (normalized by the magnification) measured at the best focus together with the corresponding simulations at the best and paraxial focus. With the achromat doublet lens, the best focus is found with the lens shifted by 150 $\mu$ m closer to the source with respect to the paraxial focus (calculated for the measured magnification of 7.39), which corresponds to a simulated magnification of 7.45. The distance between peaks decreases by 35% (from 10.9  $\mu$ m to 7.1  $\mu$ m). With the plano-convex lens, the best focus is found with the lens shifted by 200  $\mu$ m closer to the source from the paraxial focus (calculated for the measured magnification of 9.13), which corresponds to a simulated magnification of 9.30. The distance between peaks decreases by 28% (from 15.1  $\mu$ m to 10.8  $\mu$ m). The

achromat lens provides a PSF 34% smaller than the plano-convex lens.

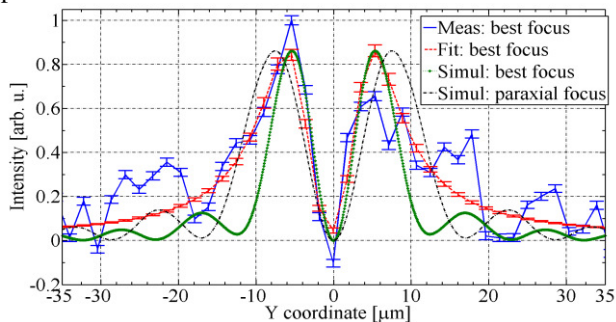


Figure 2: Vertical projection of the PSF measured with SLB-30-100-PY at the best focus and simulated at the best and at the paraxial focus.

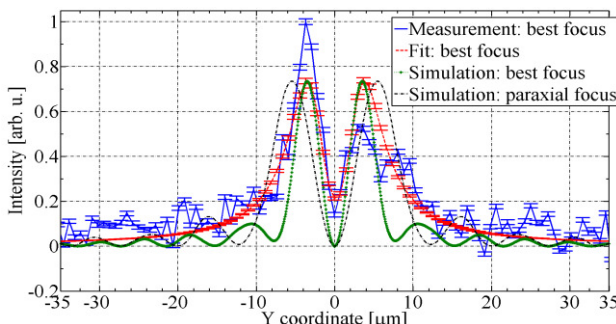


Figure 3: Vertical projection of the PSF measured with DLB-30-120-PM at the best focus and simulated at the best and at the paraxial focus.

Figure 4 shows, for the achromat doublet, the measured and simulated distance between peaks as a function of the longitudinal position of the lens. The PSF size rapidly increases as the lens is moved away from its best focus positions. Simulations and experimental data are performed in the rest of the paper at the best focus.

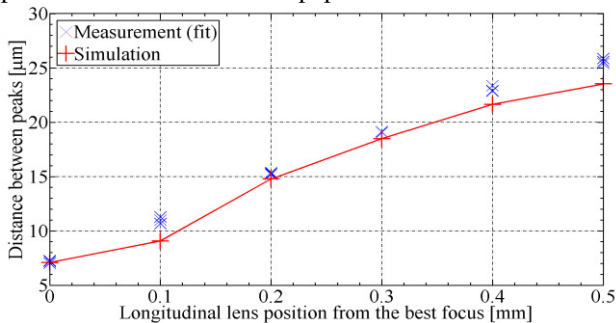


Figure 4: Distance between peaks of the OTR main lobes for different longitudinal achromat lens positions getting closer to the image from the best focus.

The evolution of the PSF of the achromat lens, measured and simulated at the best focus is presented on Fig. 5 and Fig. 6 for three different wavelengths, 500 nm, 550 nm and 600 nm. Table 1 shows the corresponding distance between peaks. Theoretical calculation expects that the diffraction effect gets smaller for shorter wavelength [1], assuming that the aberrations are kept at a very low level. Both simulations and experimental data indicate that the

size of the PSF reduces by a factor 1.5 going from 600 nm to 500 nm.

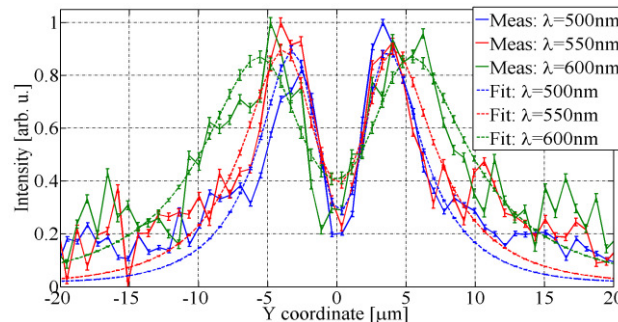


Figure 5: PSF measured at best focus for 500nm, 550nm, and 600nm wavelength optical filters (40nm bandwidth).

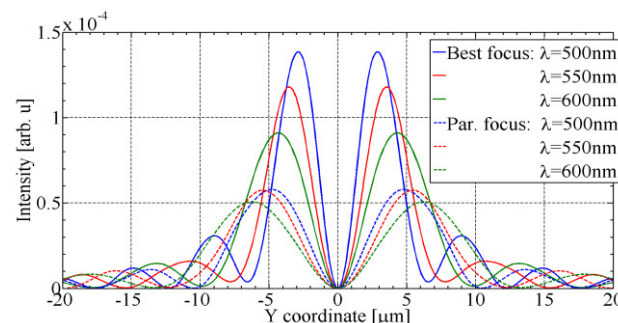


Figure 6: PSF simulated at the paraxial focus and best focus for 500nm, 550nm and 600nm wavelengths.

Table 1: Distance Between Peaks at the Best Focus for Measurements and Simulations and for Three Wavelengths

Filters	Measurements (μm)	Simulations (μm)
500 nm	6.34±0.10	5.74
550 nm	7.06±0.19	7.14
600 nm	9.89±0.26	8.65

### Chromatic Aberration

Chromatic aberrations have been studied with the achromat doublet lens by comparing the PSF measured at 550 nm wavelength filter with 40nm and 25nm bandwidth, see Fig.7. Using narrower bandpass filters do not improve the resolution but only decreases the light intensity. This is confirmed by simulations, presented in Fig. 8, which presents the expected PSF for three wavelengths 510, 550 and 590nm.

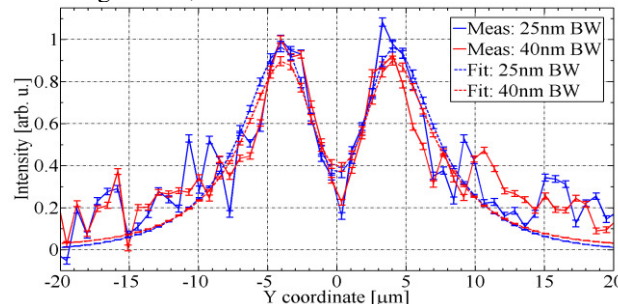


Figure 7: Projection of PSF measurements and their fit for 550nm filters of 40nm and 25nm bandwidths.

The simulations presented in Fig. 8 have been obtained with a position of the lens corresponding to the best focus condition for a 550nm wavelength. This distance was kept constant for the additional simulations performed for 510nm and 590nm wavelengths. Chromatic aberrations are thus considered not to be a limitation to the actual resolution of the monitor.

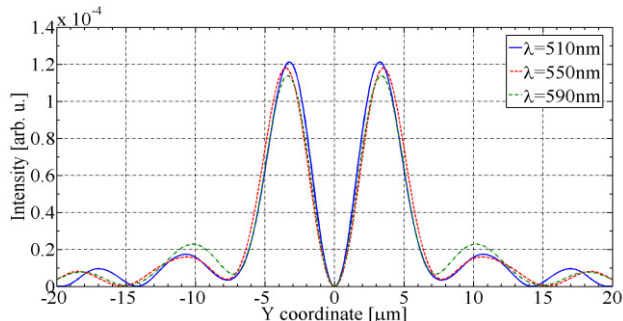


Figure 8: Projection of PSF simulations reproducing a 550nm filter of  $\pm 40$ nm bandwidth (best focus for 550nm).

### Iris Scan

An iris has been inserted at one centimetre upstream of the achromat lens to study the contribution of aberration and diffraction on the PSF. Measurements and simulations of the distance between peaks of the OTR PSF as a function of the iris diameter are presented in Fig. 9. A theoretical curve representing a typical diffraction effect (e.g. the size of an Airy disk) and which is inversely proportional to the iris diameter has been added in Fig. 9 and fitted to the simulation data in the region where we are sure that our system is diffraction limited. Below an iris diameter of 18 mm, the distance between peaks and the width of the main lobes increase due to diffraction and our system is thus completely diffraction limited. For iris diameter higher than 18 mm, the theoretical curve is slightly below the simulation data, which means that our system still suffers from small aberrations.

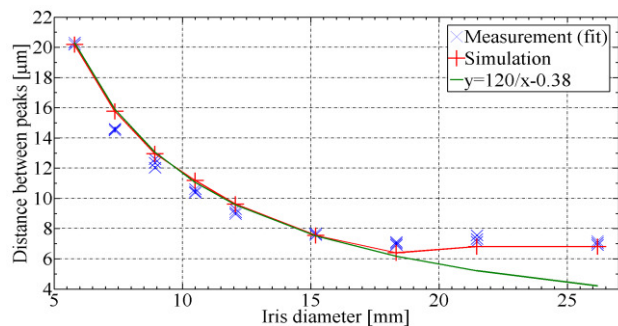


Figure 9: Distance between the two main lobes of the OTR PSF for different iris diameters.

Some examples of images measured for different iris diameters are presented in Fig. 10 in comparison with simulations. A very good agreement is found between measurements and simulations up to the micrometre scale.

Following this optimisation to provide the smallest possible PSF, the system was used to measure vertical

beam size using the visibility of the PSF. The results of the corresponding quadrupolar scan are reported here [12].

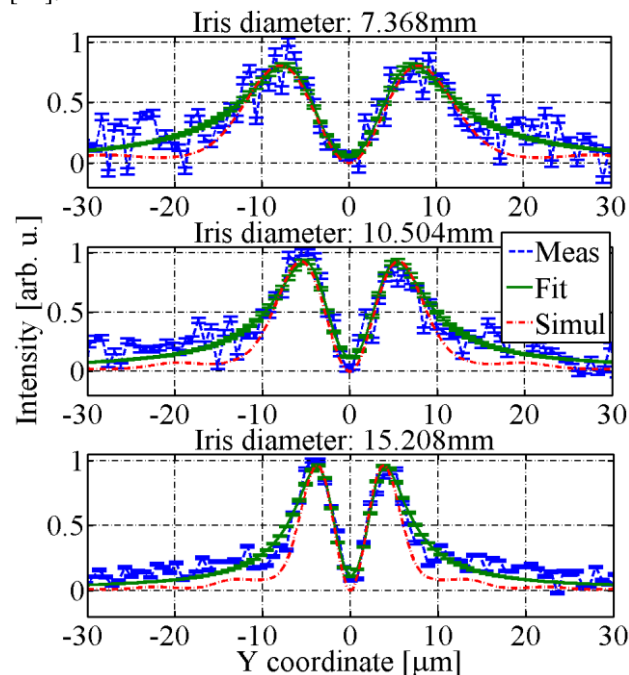


Figure 10: PSF projection measurements, fits and simulations at the best focus for different iris diameters.

## CONCLUSION

We developed simulation tools to calculate the OTR Point Spread Function using the physical optics propagation mode of ZEMAX. The code gives very accurate predictions that were compared with measurements taken at the ATF2 facility and allowed the design of an improved optical system with one of the best resolution achieved so far in beam imaging system. As future developments, we will use the code to study a possible design for beam size measurements below 300nm. The code will be improved to take into account realistic conditions that will include the key beam characteristics such as transverse dimensions, divergence and energy spread.

## REFERENCES

- [1] M. Castellano, et al., Phys Rev STAB 1, 062801 (1998)
- [2] A.P. Potylitsyn, Adv. Rad. Sources and App., Vol. 199, (2006) 149-163
- [3] P. Karataev, Phys. Lett A 345 (2005)
- [4] P. Karataev, et al., PRL 107, 174801 (2011)
- [5] A. Aryshev, et al., Journal of Physics, 236 (2010) 012008
- [6] K. Honkavaara, et al., Part.Accel. 63 (1999) 147-170
- [7] V.A. Verzilov, Phys. Lett. A 273 (2000) 135
- [8] R.A. Bosch, Nucl. Instr. and Meth. A 431 (1999) 320
- [9] Zemax User's Manual, 20th February, (2013)
- [10] M. Castellano, et al., Nuclear Instruments and Methods A 435 (1999) 297
- [11] T. Aumeyr, et al., Proc. IBIC 2013, WEPF18
- [12] K. Kruchinin, et al., Proc. IBIC 2013, WEAL2